Experimental Thermodynamics of Cluster Ions Composed of H_2SO_4 and H_2O. 2. Measurements and ab Initio Structures of Negative Ions

Karl D. Froyd[†] **and Edward R. Lovejoy***

NOAA Aeronomy Laboratory, 325 Broadway, R/AL2, Boulder, Colorado 80305

Received: December 22, 2002

Gas-phase nucleation in the atmosphere may be initiated by the condensation of sulfuric acid and water around ions. The thermodynamics of stepwise cluster ion growth must be known in order to model ion-induced nucleation of the H_2SO_4/H_2O system. In the companion paper, we measured temperature-dependent equilibrium constants for the reactions of H_2O with the $H^+(H_2SO_4)_s(H_2O)_w$ cluster ions using an ion flow reactor. In this work, H_2O bond enthalpies and entropies for the $HSO_4^-(H_2SO_4)_s(H_2O)_w$, $s \leq 6$ and $w \leq 10$, cluster ions were measured. The thermodynamics of H_2SO_4 ligand bonding in these clusters were also determined using data from previous experiments. The small positive and negative cluster ions exhibit very different chemical characteristics, but both families show trends analogous to bulk solution thermodynamics as clusters grow in size. Small negative cluster ions have a lower affinity for H_2O than positive ion species, but H_2SO_4 bonding is considerably stronger in the negative clusters. Ion-induced nucleation of the negative H_2SO_4/H_2O cluster ions is therefore thermodynamically favored. Addition of H_2O to certain $HSO_4^-(H_2SO_4)_s(H_2O)_w$ cluster ions results in unusually large reaction entropies. Ab initio calculations were performed to investigate ligand bonding in the $HSO_4^-(H_2SO_4)_s(H_2O)_w$ cluster ions. Stable cluster geometries comprised of multiple ions were identified for $s \geq 2$. Large experimental entropy changes upon H_2O addition may be due to multiply ionic species formed by proton transfer within the product cluster.

Introduction

The mechanism for new particle formation in the earth's atmosphere has not been identified. New particle production events observed in the atmosphere may be initiated by clustering around ambient ions.[1,2] Ions are likely aerosol precursors because they form very stable clusters with polar ligands. Ion-induced nucleation has been observed in the laboratory,[3−5] and modeling studies have examined cluster ion growth in aircraft and diesel engine exhaust[6] and for certain atmospheric regions.[2] However, the thermodynamics of stepwise cluster ion growth required to accurately model ion-induced nucleation over a broad range of conditions are not known. Sulfuric acid is likely to be an important component of gas-phase nucleation mechanisms,[7] and H_2SO_4 has been identified as a component of negative cluster ions in the atmosphere.[8]

In our previous laboratory study,[9,10] bond enthalpies for the pure sulfuric acid cluster ions, $HSO_4^-(H_2SO_4)_s$, $s = 1-5$, were measured. Sulfuric acid is extremely hydrophilic, and in the atmosphere, growth and nucleation of H_2SO_4-containing cluster ions would involve the uptake of water. In the present work, the equilibrium constants for the association of H_2O to the sulfuric acid clusters

$$HSO_4^-(H_2SO_4)_s(H_2O)_{w-1} + H_2O + He \rightleftarrows HSO_4^-(H_2SO_4)_s(H_2O)_w + He \quad (1)$$

were measured over a range of temperatures, and bond enthalpies and entropies were determined. Ab initio calculations of these cluster ions were performed to explore H_2O ligand bonding and to elucidate experimental thermodynamic results. The accompanying article (part 1)[11] describes thermodynamic measurements of the analogous positive ion system, $H^+(H_2SO_4)_s(H_2O)_w$. The positive and negative systems are compared at the end of this work, and the role of H_2SO_4/H_2O cluster ions as potential ion-induced nucleation precursors is discussed.

Experimental Method

Cluster ion thermodynamics were measured using an ion flow reactor coupled to a quadrupole mass spectrometer. The details of this system are given in part 1.[11] Briefly, positive and negative ions were generated at the upstream end of a temperature-controlled, low pressure, laminar flow reactor. Water and sulfuric acid vapor introduced into the system reacted with primary ions to create stable secondary ions, which then reacted with neutral molecules in the presence of helium carrier gas to produce cluster ions. The predominant negative cluster ion family was of the form $HSO_4^-(H_2SO_4)_s(H_2O)_w$, where s and w correspond to the number of H_2SO_4 and H_2O ligands, respectively. Cluster ions were in chemical equilibrium with a known concentration of gas-phase H_2O. Negative ions and neutral molecules were sampled into a vacuum chamber at the downstream end of the reactor, where ions were focused and collimated with a set of electrostatic lenses and detected with a quadrupole mass spectrometer. Ion signal ratios and the absolute concentration of gas-phase water were used to determine equilibrium constants, K_p, for reaction 1. A van't Hoff analysis of equilibrium constants measured over a range of reactor temperatures yielded H_2O bond enthalpies and entropies, $\Delta H°$ and $\Delta S°$, for the $HSO_4^-(H_2SO_4)_s(H_2O)_w$ cluster ions.

* To whom correspondence should be addressed. E-mail: nlovejoy@al.noaa.gov.

[†] Also affiliated with the Cooperative Institute for Research in Environmental Sciences, and the Department of Chemistry and Biochemistry at the University of Colorado, Boulder, Colorado 80309.

10.1021/jp0278059 CCC: $25.00
Published on Web 10/29/2003

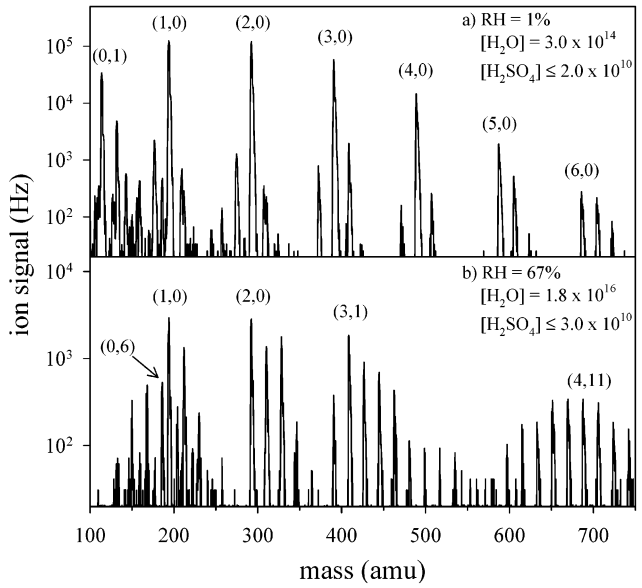

Figure 1. Mass spectra of $HSO_4^-(H_2SO_4)_s(H_2O)_w$, $s = 0-6$, recorded at a flow reactor temperature of 252 K. The relative humidity with respect to ice is listed, and H_2O and H_2SO_4 concentrations are given in molecule cm^{-3}. The most intense cluster ion peak in each H_2O envelope is labeled $(s,w) \equiv HSO_4^-(H_2SO_4)_s(H_2O)_w$.

Results

Cluster Ion Mass Spectra. Mass spectra for the $HSO_4^-(H_2SO_4)_s(H_2O)_w$ cluster ion family at 252 K are shown in Figure 1 for two concentrations of H_2O. With concentrations of $[H_2SO_4] \leq 2.0 \times 10^{10}$ molecule cm^{-3} in spectrum (a), ions with as many as 6 H_2SO_4 ligands are observed. At a relative humidity of 1%, the dominant peak in each H_2SO_4 envelope ($s = 1-6$) is the unhydrated $HSO_4^-(H_2SO_4)_s$ cluster, but the H_2O equilibrium distributions suggest that the affinity for H_2O increases for the larger H_2SO_4 clusters. At a higher relative humidity of 67% in (b), the $HSO_4^-(H_2SO_4)_s(H_2O)_w$ clusters acquire several H_2O ligands. The HSO_4^- core ion is relatively hydrophilic, with 6 H_2O ligands at the peak of the distribution. The affinity for H_2O drops dramatically when the first H_2SO_4 molecule is added. The $s = 3$ series characterizes a transition between small clusters, which have a low affinity for H_2O and the more hydrophilic $s = 4$, 5, and 6 clusters. The $s = 3$ envelope is divided into two modes, one at $w = 1-4$ where peak ratios indicate rapidly falling H_2O affinity and $w \geq 5$ clusters which more readily bind H_2O, indicated by consistent ~1:1 peak ratios. The most abundant clusters in each H_2O distribution are $HSO_4^-(H_2SO_4)$, $HSO_4^-(H_2SO_4)_2$, $HSO_4^-(H_2SO_4)_3(H_2O)$, and $HSO_4^-(H_2SO_4)_4(H_2O)_{11}$, exemplifying the abrupt increase in H_2O affinity from $s = 3$ to 4. A dramatic widening of the H_2O distributions over $HSO_4^-(H_2SO_4)_s$ also occurs as s increases. Comparing spectra in Figure 1 with those of the $H^+(H_2SO_4)_s(H_2O)_w$ clusters,[11] it is clear that negative H_2SO_4/H_2O cluster ions have a significantly lower affinity for H_2O than the corresponding positive ion family.

Thermodynamic Measurements. Measurements of $HSO_4^-(H_2SO_4)_s(H_2O)_w$ cluster ion equilibria with H_2O via reaction 1 were performed at reactor temperatures of 218−273 K and pressures of 0.8−18 Torr. Cylindrical, 5/8″ diameter quadrupole rods were employed for the study of clusters with 0, 1, 2, and 3 H_2SO_4 molecules. Additional measurements were later made for the $s = 3-6$ clusters using 1/2″ diameter quadrupole rods with an extended mass range. Results for the $s = 3$ clusters obtained using the two mass filters were indistinguishable within experimental precision over the entire temperature range. Van't Hoff plots for the $HSO_4^-(H_2O)_w$ and $HSO_4^-(H_2SO_4)_3(H_2O)_w$ cluster ions are shown in Figure 2. Experimental thermodynamic results are summarized in Table 1. Total uncertainties in $\Delta G°$ values, representing both precision and systematic error, are estimated to be approximately ±1 kcal mol^{-1}.

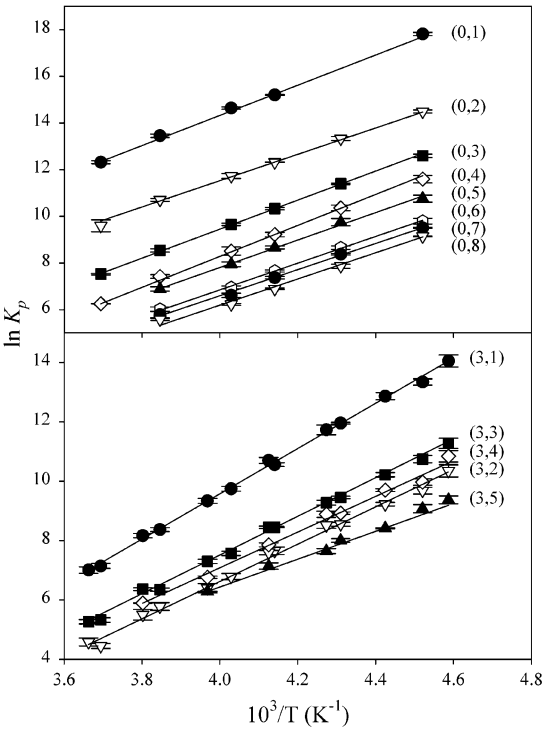

Figure 2. Van't Hoff plots for association of H_2O to form the $HSO_4^-(H_2O)_w$, $w = 1-8$, and $HSO_4^-(H_2SO_4)_3(H_2O)_w$, $w = 1-5$, cluster ions via reaction 1. Product clusters are labeled (s,w). Points represent the average of from 2 to 24 individual measurements of the equilibrium constant, and error bars are one standard deviation of ln K_p. Lines are weighted, linear least-squares fits to the data, where points are weighted by the inverse square of the standard deviation.

The mass spectrum in Figure 1a was recorded under relatively low H_2O and high H_2SO_4 concentrations. The peaks located 18 mass units lower than the $HSO_4^-(H_2SO_4)_s$ peaks are identified as $HSO_4^-(H_2SO_4)_s(SO_3)$. The SO_3 vapor pressure over the H_2SO_4/H_2O liquid source was ~500−50000 times lower than the H_2SO_4 pressure.[12] However, thermal decomposition experiments of $HSO_4^-(H_2SO_4)_s(SO_3)$ performed in our laboratory show that the SO_3 ligand bond strength is comparable to that of H_2SO_4.[13] Signal intensities for ions containing SO_3 were generally more than 100 times smaller than $HSO_4^-(H_2SO_4)_s(H_2O)_w$ signals, and SO_3 peaks were observed in the mass spectrum only when H_2SO_4 was unusually high and very little gas-phase H_2O was present. It is likely that $HSO_4^-(H_2SO_4)_s(SO_3)$ clusters also acquire H_2O ligands

$$HSO_4^-(H_2SO_4)_s(SO_3)(H_2O)_{w-1} + H_2O \rightleftarrows HSO_4^-(H_2SO_4)_s(SO_3)(H_2O)_w \quad (2)$$

The product clusters of reaction 2 have the same mass as $HSO_4^-(H_2SO_4)_{s+1}(H_2O)_{w-1}$, and these interfering signals would lead to a variation in the measured $\Delta G°$ values over a range of H_2O concentrations.[11] SO_3 and H_2O within a cluster may also isomerize to form H_2SO_4

$$HSO_4^-(H_2SO_4)_s(SO_3)(H_2O) \rightarrow HSO_4^-(H_2SO_4)_{s+1} \quad (3)$$

further complicating the equilibrium measurement. It was found

TABLE 1: Thermodynamic Results for the Reactions, $HSO_4^-(H_2SO_4)_s(H_2O)_{w-1} + H_2O \rightleftarrows HSO_4^-(H_2SO_4)_s(H_2O)_w$ for $s = 0-6$[a]

T	(0,1)	(0,2)	(0,3)	(0,4)	(0,5)	(0,6)	(0,7)	(0,8)	T	(1,1)	(1,2)	(1,3)
	−7.83[b]	−6.37	−5.54	−5.10	−4.73	−4.31	−4.18	−4.02		−3.97[b]	−3.58	
221	0.03[c]	0.03	0.03	0.07	0.07	0.05	0.01	0.01	221	0.03[c]	0.05	
	2[d]	6	14	18	16	14	10	4		18[d]	16	
		−6.15	−5.25	−4.78	−4.50	−3.99	−3.86	−3.63		−3.80	−3.33	−3.27
232		0.04	0.01	0.05	0.07	0.03	0.01	0.04	232	0.05	0.05	0.04
		2	4	10	10	8	6	2		10	10	2
	−7.30	−5.91	−4.96	−4.42	−4.16	−3.68	−3.54	−3.31		−3.58	−3.09	−2.97
242	0.01	0.01	0.03	0.04	0.03	0.02	0.02	0.01	242	0.05	0.02	0.01
	6	6	10	14	12	8	6	4		16	8	4
	−7.22	−5.78	−4.76	−4.20	−3.92	−3.43	−3.26	−3.07		−3.43	−2.85	−2.78
248	0.02	0.05	0.02	0.09	0.05	0.03	0.05	0.02	248	0.02	0.03	0.04
	6	8	12	12	12	8	8	6		20	10	6
	−6.95	−5.53	−4.41	−3.83	−3.56	−3.11	−2.99	−2.88		−3.16	−2.61	−2.33
260	0.04	0.03	0.04	0.04	0.05	0.05	0.07	0.02	260	0.08	0.04	0.04
	6	12	18	14	12	8	8	6		18	8	6
	−6.63	−5.16	−4.05	−3.36						−2.91	−2.29	
271	0.03	0.14	0.02	0.01					271	0.06	0.00	
	4	8	6	4						10	4	
$\Delta H°$	−12.9	−11.2	−12.4	−13.2	−11.7	−11.4	−11.1	−11.2	$\Delta H°$	−8.7	−9.5	−11.1
σ	0.2	0.2	0.1	0.2	0.5	0.4	0.2	0.1	σ	0.3	0.1	0.5
95% CI	0.6	0.7	0.4	0.6	1.5	1.2	0.7	0.3	95% CI	0.7	0.4	2.0
$\Delta S°$	−23.0	−22.0	−30.7	−36.3	−31.2	−31.8	−31.4	−32.3	$\Delta S°$	−21.1	−26.5	−33.5
σ	0.8	1.0	0.5	0.8	2.0	1.5	0.9	0.5	σ	1.1	0.5	1.9
95% CI	2.7	2.7	1.4	2.2	6.3	4.9	2.9	1.5	95% CI	3.0	1.5	8.3

T	(2,1)	(2,2)	(2,3)	(2,4)	T	(3,1)	(3,2)	(3,3)	(3,4)	(3,5)	(3,6)	(3,7)	(3,8)	(3,9)
	−4.23[b]	−5.03	−3.51	−3.71		−6.09[b]	−4.48	−4.89	−4.70	−4.06	−4.53	−4.73	−4.98	−4.70
221	0.04[c]	0.04	0.04	0.03	218	0.09[c]	0.09	0.07	0.08	0.06	0.07	0.05	0.05	0.03
	18[d]	16	14	2		14[d]	14	14	14	14	8	6	6	6
	−3.97	−4.66	−3.20	−3.42		−5.86	−4.26	−4.72	−4.38	−3.99				
232	0.03	0.08	0.04	0.01	221	0.05	0.05	0.05	0.05	0.06				
	10	10	8	4		18	16	16	14	6				
	−3.61	−4.22	−2.86	−3.07		−5.78	−4.14	−4.59	−4.36	−3.78	−4.27	−4.43	−4.75	−4.31
242	0.09	0.07	0.02	0.01	226	0.05	0.03	0.03	0.02	0.01	0.04	0.01	0.03	0.04
	16	12	8	4		16	16	16	12	6	6	4	4	4
	−3.37	−4.01	−2.60	−2.86		−5.51	−3.94	−4.36	−4.12	−3.69				
248	0.08	0.10	0.03	0.03	232	0.01	0.03	0.02	0.02	0.03				
	14	12	8	8		10	10	10	8	6				
	−3.02	−3.57	−2.29	−2.47		−5.45	−3.96	−4.31	−4.13	−3.56	−4.05	−4.23	−4.45	−4.12
260	0.06	0.02	0.07	0.02	234	0.08	0.05	0.04	0.05	0.04	0.04	0.07	0.03	0.09
	14	12	6	4		18	18	14	10	4	4	4	4	4
	−2.58	−3.06				−5.07	−3.67	−4.06						
271	0.07	0.04			242	0.03	0.06	0.01						
	10	6				14	10	8						
$\Delta H°$	−11.7	−13.6	−10.9	−11.3		−5.15	−3.66	−4.07	−3.78	−3.44	−3.87	−3.98	−4.21	−3.87
σ	0.3	0.2	0.4	0.2	242	0.05	0.03	0.02	0.03	0.05	0.01	0.01	0.06	0.01
95% CI	0.9	0.7	1.3	0.5		18	18	10	8	6	4	4	4	4
$\Delta S°$	−33.5	−38.6	−33.2	−33.9		−4.81	−3.35	−3.73						
σ	1.4	1.0	1.6	0.7	248	0.04	0.05	0.04						
95% CI	3.8	2.7	5.2	2.2		16	12	10						
						−4.68	−3.20	−3.65	−3.39	−3.15	−3.52			
					252	0.04	0.08	0.04	0.02	0.01	0.04			
						26	24	14	10	4	2			
						−4.32	−2.99	−3.28						
					260	0.03	0.07	0.03						
						14	12	8						
						−4.27	−2.88	−3.33	−3.08					
					263	0.04	0.09	0.02	0.00					
						16	12	8	4					
						−3.84	−2.40	−2.87						
					271	0.04	0.04	0.04						
						8	4	2						
						−3.80	−2.49	−2.86						
					273	0.06	0.07	0.04						
						14	12	6						
					$\Delta H°$	−15.1	−12.5	−12.9	−11.9	−9.3	−10.4	−10.6	−12.3	−11.7
					σ	0.2	0.2	0.1	0.1	0.1	0.4	0.2	0.6	0.3
					95% CI	0.4	0.4	0.3	0.2	0.2	1.2	1.0	2.7	1.1
					$\Delta S°$	−41.5	−36.8	−36.8	−33.7	−24.5	−26.8	−27.5	−33.5	−32.4
					σ	0.7	0.8	0.6	0.4	0.4	1.6	1.0	2.7	1.0
					95% CI	1.5	1.8	1.2	0.9	0.9	5.2	4.2	11.6	4.5

TABLE 1: (Continued)

T	(4,1)	(4,2)	(4,3)	(4,4)	(4,5)	(4,6)	(4,7)	(4,8)	(4,9)	(4,10)
	−5.91[b]	−5.81	−5.55	−5.26	−4.94	−5.22	−5.47	−5.06	−5.27	−5.07
218	0.00[c]	0.09	0.05	0.08	0.06	0.04	0.07	0.05	0.05	0.07
	4[d]	8	8	8	8	10	10	10	12	12
	−5.51	−5.47	−5.20	−4.86	−4.61	−4.85	−4.97	−4.76	−4.94	−4.62
226	0.05	0.06	0.05	0.06	0.04	0.06	0.02	0.05	0.05	0.02
	10	10	10	10	12	8	8	12	12	10
	−5.25	−5.23	−4.95	−4.60	−4.35	−4.60	−4.71	−4.54	−4.63	−4.38
234	0.07	0.05	0.06	0.04	0.03	0.02	0.01	0.03	0.06	0.01
	14	14	14	10	6	6	6	8	8	6
	−4.94	−4.99	−4.67	−4.36	−4.16	−4.35	−4.52	−4.17	−4.37	−4.19
242	0.06	0.03	0.05	0.02	0.04	0.05	0.01	0.02	0.02	0.02
	12	14	14	8	6	6	6	4	6	8
	−4.48	−4.52	−4.25	−3.90	−3.78	−3.97	−4.00	−3.80	−3.97	−3.73
252	0.09	0.05	0.04	0.05	0.05	0.04	0.03	0.05	0.05	0.01
	24	22	20	12	10	10	10	10	10	4
	−4.06	−4.18	−3.85	−3.57	−3.43	−3.59	−3.55	−3.43	−3.56	−3.28
263	0.13	0.04	0.03	0.05	0.02	0.01	0.03	0.04	0.03	0.03
	16	14	10	10	8	6	4	4	2	2
	−3.56	−3.77	−3.38	−3.12	−3.03					
273	0.14	0.02	0.02	0.01	0.03					
	14	14	8	6	4					
$\Delta H°$	−15.1	−14.0	−14.1	−13.8	−12.2	−12.8	−13.3	−13.1	−13.5	−12.7
σ	0.3	0.2	0.2	0.1	0.2	0.2	0.2	0.3	0.3	0.1
95% CI	0.7	0.5	0.5	0.3	0.5	0.4	0.5	0.8	0.7	0.4
$\Delta S°$	−41.9	−37.6	−39.2	−39.1	−33.6	−35.2	−36.8	−36.8	−37.7	−35.7
σ	1.2	0.8	0.8	0.5	0.7	0.6	0.8	1.2	1.1	0.6
95% CI	3.2	2.0	2.0	1.3	1.8	1.7	2.1	3.3	3.0	1.6

T	(5,1)	(5,2)	(5,3)	(5,4)	(5,5)	(5,6)	(5,7)	(5,8)	(5,9)	(5,10)
					−5.62[b]	−5.67	−5.68	−5.63	−5.25	−5.41
218					0.04[c]	0.04	0.02	0.11	0.05	0.04
					2[d]	2	4	6	8	8
		−6.02	−5.68	−5.40	−5.29	−5.44	−5.29	−5.22	−4.97	−5.04
226		0.01	0.01	0.04	0.10	0.06	0.03	0.06	0.06	0.11
		4	6	6	8	8	8	4	6	6
	−6.62	−5.73	−5.40	−5.08	−5.07	−5.11	−4.94	−4.96	−4.62	−4.74
234	0.03	0.04	0.04	0.04	0.10	0.03	0.02	0.02	0.04	0.06
	6	10	10	10	8	8	6	6	6	6
	−6.26	−5.41	−5.16	−4.85	−4.83	−4.83	−4.65	−4.72	−4.30	−4.37
242	0.04	0.03	0.05	0.05	0.08	0.01	0.02	0.08	0.01	0.03
	8	8	10	10	6	4	4	6	6	4
	−5.73	−4.97	−4.62	−4.38	−4.41	−4.39	−4.20	−4.26	−3.94	−4.04
252	0.04	0.03	0.05	0.07	0.03	0.05	0.01	0.02	0.00	0.07
	8	12	10	14	10	6	6	8	6	8
	−5.27	−4.52	−4.36	−4.11	−4.03	−4.00	−3.88	−3.91	−3.60	−3.70
263	0.03	0.07	0.06	0.09	0.02	0.04	0.03	0.04	0.06	0.04
	10	12	8	8	8	8	8	8	6	4
	−4.74	−4.06	−3.91	−3.71	−3.64	−3.59	−3.47	−3.54		
273	0.02	0.05	0.01	0.06	0.03	0.01	0.06	0.03		
	10	14	8	8	6	6	4	2		
$\Delta H°$	−17.9	−15.3	−14.2	−13.5	−13.4	−14.6	−14.6	−13.5	−13.5	−13.7
σ	0.2	0.2	0.1	0.3	0.2	0.1	0.1	0.2	0.2	0.3
95% CI	0.6	0.5	0.2	0.9	0.5	0.2	0.3	0.5	0.6	0.8
$\Delta S°$	−48.4	−40.9	−37.5	−35.8	−35.8	−40.2	−41.3	−36.6	−38.0	−38.1
σ	0.8	0.8	0.3	1.3	0.8	0.3	0.6	0.8	0.8	1.2
95% CI	2.5	2.3	0.9	3.7	2.0	0.8	1.4	2.1	2.3	3.3

T	(6,1)	(6,2)	(6,3)	(6,4)
			−5.93[b]	−5.75
234			0.04[c]	0.04
			2[d]	2
	−6.89	−6.14	−5.51	−5.39
242	0.01	0.07	0.03	0.04
	4	6	8	6
	−6.35	−5.58	−5.07	−4.95
252	0.03	0.04	0.03	0.03
	2	4	6	6
	−5.82	−5.15	−4.60	−4.58
263	0.04	0.03	0.03	0.00
	6	8	8	4
	−5.27	−4.66	−4.24	−4.28
273	0.10	0.01	0.04	0.06
	6	4	6	4
$\Delta H°$	−19.7	−17.3	−16.0	−14.8
σ	0.4	0.4	0.3	0.3
95% CI	1.7	1.5	0.9	0.8
$\Delta S°$	−53.0	−46.4	−43.2	−38.9
σ	1.6	1.3	1.2	1.0
95% CI	7.1	5.6	3.7	3.2

[a] Product clusters are labeled (*s*,*w*). Values for each cluster correspond to [b]$\Delta G°$, [c]the standard deviation, and [d]the number of measurements. $\Delta H°$ and $\Delta S°$ values are listed along with standard deviations and 95% confidence intervals for the fits to the van't Hoff equation. $\Delta G°$ and $\Delta H°$ are given in units of kcal mol^{-1} and $\Delta S°$ is in cal mol^{-1} K^{-1}.

that SO_3 peaks in the mass spectrum could be almost entirely removed by adding liquid water to the sulfuric acid source and lowering its temperature to <330 K, thereby reducing the SO_3 vapor pressure relative to that of H_2SO_4. To a lesser extent, SO_3 peaks were also removed by adding gas-phase H_2O to the flow reactor, suggesting that either gas-phase SO_3 was converted to H_2SO_4 or that $HSO_4^-(H_2SO_4)_s(SO_3)$ cluster ions were hydrated via reaction 2. Signatures corresponding to SO_3 were not observed in $H^+(H_2SO_4)_s(H_2O)_w$ mass spectra.

Measurements of $\Delta G°$ for formation of $HSO_4^-(H_2SO_4)_s(H_2O)_w$ via reaction 1 were generally independent of $[H_2O]$ over a wide range, demonstrating that cluster ions were in equilibrium with H_2O and that background interference signals (due to SO_3 or other contaminants), sampling complications, and ion loss processes exhibited a negligible effect on the experimental results (see part 1).[11] Figure 3 shows $\Delta G°$ measured at 242 and 273 K over a range of H_2O concentrations for several cluster ions. $\Delta G°$ values varied most sharply for the $HSO_4^-(H_2SO_4)_4(H_2O)$ cluster, decreasing by up to 0.3 kcal mol^{-1} as $[H_2O]$ increased by a factor of 20. This trend was most pronounced at reactor temperatures >250 K where SO_3 was observed in the mass spectra, suggesting that the H_2SO_4 and

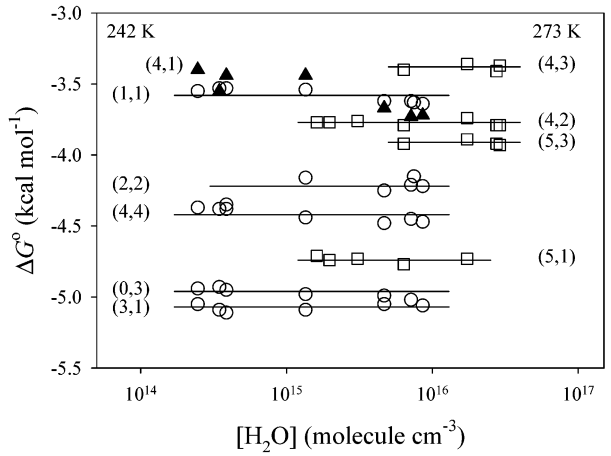

Figure 3. Variation of experimental $\Delta G°$ values for reaction 1 measured at various concentrations of H_2O in the flow reactor. Representative results for the formation of $HSO_4^-(H_2SO_4)_s(H_2O)_w$ clusters at 242 K (open circles) and 273 K (open squares) are shown, where product clusters are labeled (*s*,*w*). The filled triangles are results for the $HSO_4^-(H_2SO_4)_4(H_2O)$ cluster ion at 273 K. Lines are average $\Delta G°$ values.

SO_3 equilibrium reactions 1 and 2 were happening concurrently, resulting in a $HSO_4^-(H_2SO_4)_3(SO_3)(H_2O)_2$ signal coincident with $HSO_4^-(H_2SO_4)_4(H_2O)$. The signal intensities of $HSO_4^-(H_2SO_4)_3(SO_3)$ were <10% of $HSO_4^-(H_2SO_4)_4$, and the variation in $\Delta G°$ with $[H_2O]$ for formation of $HSO_4^-(H_2SO_4)_4(H_2O)$ was near typical experimental precision. Therefore, uncorrected average $\Delta G°$ values are reported for all clusters.

Cluster ions may undergo unimolecular decomposition in the high vacuum region during ion analysis.[14,15] The unimolecular decomposition rate constant increases with temperature, and temperature-dependent shifts in the cluster ion distribution due to decomposition during sampling are not easily distinguished from the temperature dependence of equilibrium reaction 1. In such a case, a van't Hoff analysis of the apparent equilibrium constants may lead to values of $\Delta H°$ and $\Delta S°$ for H_2O association that are anomalously negative. Sunner and Kebarle[15] used binding energies and vibrational frequencies calculated with an electrostatic technique to determine RRKM unimolecular decomposition rate constants, $k(E)$, for the $K^+(H_2O)_w$ cluster ions. They found that significant decomposition occurred in their mass analysis system for $w > 4$. To avoid decomposition, they recommended that cluster equilibrium measurements be performed at the lowest accessible temperatures, such that $K_{w-1,w} > 10$ Torr^{-1}. The majority of the equilibrium constants measured in the current work conform to this limit. However, a more rigorous investigation was undertaken to determine the extent of unimolecular decomposition for the $HSO_4^-(H_2SO_4)_s(H_2O)_w$ cluster ions.

The microcanonical, unimolecular decomposition rate constant depends on the density of states of the reactant ion, $\rho(E)$, and the number of accessible reaction channels at the transition state, $N(E)$

$$k(E) = \frac{N(E)}{\hbar\rho(E)} \tag{4}$$

The density of states is a strong function of internal energy, and large and/or strongly bound clusters have much higher values of $\rho(E)$ at the dissociation threshold, E_d. However, $N(E)$ also increases sharply with energy, and at some energy above E_d, unimolecular decomposition of cluster ions will become sufficiently rapid to occur on experimental time scales. Ion flight times through the electrostatic lenses and quadrupole filter are on the order of ~50 μs so that only values of $k(E) > 10^4$ s^{-1} will result in significant ion decomposition. States that have decomposition rate coefficients, $k(E)$, greater than the collision rate coefficient in the flow reactor will have negligible populations because these states decompose faster than they are populated by collisions of the carrier gas. Typical collision rate coefficients in the flow reactor are $(0.5-5) \times 10^8$ s^{-1}, and thus, states with $k(E) > 10^8$ s^{-1} have negligible steady state populations in the experimental apparatus. Therefore, for the conditions of the present study, ion signal intensities will not accurately reflect ion concentrations in the flow reactor for clusters that decompose with rate coefficients between 10^4 and 10^8 s^{-1}.

To evaluate cluster ion decomposition during mass analysis, we employed a kinetic master equation model developed by Lovejoy and Curtius.[10] Ab initio vibrational frequencies, rotational constants, and experimental bond enthalpies were used to calculate $k(E)$ values above the dissociation threshold at various experimental temperatures. Boltzmann distributions were calculated for clusters in the flow reactor to determine the relative state populations at energies where unimolecular decomposition during sampling was important (i.e., $k(E) = 10^4-10^8$ s^{-1}). For some clusters, frequencies and rotational constants were extrapolated from ab initio results based on the methods of Curtius et al.[9] The $HSO_4^-(H_2SO_4)(H_2O)$ cluster ion has a dissociation energy of $E_d \approx \Delta H° = 8.7$ kcal mol^{-1}, and $k(E)$ increases sharply above this energy. At 271 K, the highest experimental measurement temperature for this cluster, only 6% of the thermal population exists in the energy range where $k(E) = 10^4-10^8$ s^{-1}. The low average vibrational energy of the $HSO_4^-(H_2SO_4)(H_2O)$ cluster ion ($E_{vib} = 5.1$ kcal mol^{-1}) limits the thermal population above its dissociation threshold, and there is little overall decomposition in the vacuum region. For the much larger $HSO_4^-(H_2SO_4)_5(H_2O)$ cluster ion at 273 K, $E_d \approx 18.0$ kcal mol^{-1} and $E_{vib} = 18.8$ kcal mol^{-1} so that nearly half of the thermal population is above the dissociation threshold. The relevant $k(E)$ window (10^4-10^8 s^{-1}) spans a wide energy range, $E = 25.8-34.0$ kcal mol^{-1}, but only 8% of the total $HSO_4^-(H_2SO_4)_5(H_2O)$ ion population exists within this range. The $HSO_4^-(H_2SO_4)_5(H_2O)$ cluster ion is large and quite stable, and $k(E)$ values only exceed 10^4 s^{-1} at energies >7 kcal mol^{-1} above E_d. Significant unimolecular decomposition is predicted, however, for $HSO_4^-(H_2SO_4)_3(H_2O)_5$, a relatively large and weakly bound cluster ion. At 252 K, it is predicted that 77% of the sampled ions decompose before they are detected. Decomposition subsides at lower temperatures, but even at 218 K, 42% of these clusters fall apart in the vacuum region. Both the $HSO_4^-(H_2SO_4)_3(H_2O)_4$ and $HSO_4^-(H_2SO_4)_3(H_2O)_6$ cluster ions also undergo significant decomposition (24% and 64%, respectively, at 252 K). To examine the effect of cluster decomposition on the thermochemical results, decomposition estimates were used to adjust experimental $\Delta G°$ values for the $HSO_4^-(H_2SO_4)_3(H_2O)_5$ cluster ion. Because the adjacent cluster ions also decompose similarly, errors in the measured thermochemical parameters for $HSO_4^-(H_2SO_4)_3(H_2O)_5$ are largely offset. The correction to $\Delta G°$ was only ~0.2 kcal mol^{-1} and nearly constant over all temperatures. Corrections to $\Delta H°$ and $\Delta S°$ were <0.1 kcal mol^{-1} and <1 cal mol^{-1} K^{-1}, respectively. In general, significant unimolecular decomposition is predicted for large, weakly bound $HSO_4^-(H_2SO_4)_s(H_2O)_w$ cluster ions during mass analysis, effectively shifting the H_2O distribution from w to $w-1$. However, simulations indicate that the thermochemical

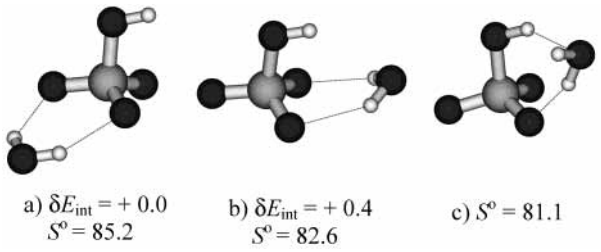

Figure 4. Convergent structures of the $HSO_4^-(H_2O)$ cluster ion. Relative energies, δE_{int}, are shown in kcal mol^{-1} and absolute entropy values at 246 K, $S°$, are in cal mol^{-1} K^{-1}. Structures a and b were calculated at the HF/6-31+G(d) level, whereas structure c was generated using B3LYP/6-31+G(d) density functional theory. The entropy for structure c was determined using unscaled vibrational frequencies.

results of this study are not greatly affected, and final $\Delta G°$, $\Delta H°$, and $\Delta S°$ values for all reactions are presented without adjustment.

Ab Initio Calculations. Numerous theoretical studies have investigated hydrogen bonding in small ionic clusters containing H_2O.[16] Structures for the $HSO_4^-(H_2SO_4)_s$ cluster ions were calculated in our earlier work[9] for $s = 0-4$. Three research groups have investigated structural trends in neutral sulfuric acid hydrates, $H_2SO_4(H_2O)_w$, using density functional theory. Arstila et al.[17] first published structures of $H_2SO_4(H_2O)_w$, $w = 0-3$ using a valence-only basis set. Higher level B3LYP calculations were performed by Bandy and Ianni[18] for $w = 0-7$ and by Re et al.[19] for $w = 0-5$. The latter two studies investigated proton-transfer isomerizations within these $H_2SO_4(H_2O)_w$ clusters. In the present study, ab initio calculations were performed for the $HSO_4^-(H_2SO_4)_s(H_2O)_w$ cluster ion family to investigate structural aspects of H_2O ligand bonding. Although computational expense limited the current study to relatively low levels of theory, the HF method employed is expected to produce qualitatively accurate geometries, and the structures presented here provide a framework for further theoretical investigations using more accurate methods. The GAMESS ab initio package[20] was used for all structure calculations. Geometry optimizations and calculations of the force constant matrix were performed at the HF/6-31+G(d) level. A maximum gradient tolerance of $<(2-10) \times 10^{-6}$ Hartree/Bohr on the potential energy surface was required to attain convergence, and a consistent set of RHF integral control parameters was used for calculating final geometries. Molecular structures were built and visualized with Molden.[21]

We attempted to identify the global minimum structures for the $HSO_4^-(H_2SO_4)_s(H_2O)_w$ cluster ions, $s \leq 3$ and $w \leq 2$. Geometry optimization routines were initiated with multiple starting geometries constructed based on chemical intuition and attempts to both maximize the number of hydrogen bonds and create favorable hydrogen bonding geometries. Converged structures are shown in Figures 4−8, and Cartesian coordinates, vibrational frequencies, and rotational constants are provided as Supporting Information. Calculated thermochemical results are listed in Table 2. The total thermal cluster energy, E, was determined from ab initio molecular properties as follows:

$$E = E_{int} + E_{vib} + E_{rot} + E_{trans} \quad (5)$$

$$E_{int} = E_e + E_{ZP} \quad (6)$$

In the above equations, E_e, E_{vib}, E_{rot}, and E_{trans} are the electronic, vibrational, rotational, and translational energies, and E_{ZP} is the vibrational zero-point energy. The stabilities of isomeric forms of a cluster ion are compared in terms of their internal energy relative to the most stable isomer, δE_{int}. Energy, enthalpy, and entropy values were calculated from standard statistical mechanics formulas[22] using ab initio harmonic oscillator vibrational frequencies and rigid rotor rotational constants. Vibrational frequencies were scaled by a factor of 0.89 to correct for systematic error in the HF method.[23] Thermochemical parameters were calculated at 246 K, corresponding to the mean temperature of experimental equilibrium measurements. Hydrogen bonding geometries of the H_2O ligands in the cluster ions are described as (d(O−H), ∠(O−H···O), d(H···O)). In this work, stronger hydrogen linkages are generally indicated by elongated covalent O−H bonds, d(O−H) > about 0.98 Å, nearly collinear geometries, ∠O−H···O ≈ 170−180°, and shorter intermolecular bond distances, d(H···O) < about 1.9 Å.

$HSO_4^-(H_2O)$. Three conformations of the $HSO_4^-(H_2O)$ cluster ion are presented in Figure 4. The isomer in Figure 4b is a C_s symmetric structure with two equivalent weak hydrogen bonds (0.95, 137, 2.19) connecting the hydrogen atoms on H_2O with the oxygens on the HSO_4^-. This conformation has the lowest electronic energy, E_e, but structure 4a, with two very similar hydrogen bonds, (0.95, 144, 2.18) and (0.95, 140, 2.24), has a slightly lower overall internal energy, E_{int}. These two isomers are energetically indistinguishable within the uncertainty of the method. The lowest frequency vibrational modes of structure 4b are H_2O torsional motions. The torsional frequencies of structure 4b are slightly higher than those in 4a because of the interaction of the H_2O oxygen with the hydrogen on HSO_4^-, lowering the entropy of structure b relative to that of a. The doubly linked $HSO_4^-(H_2O)$ structure 4c was first calculated by Arstila et al.[17] using the DFT-BLYP method. Bandy and Ianni[18] and Re et al.[19] also observe this same type of linkage between neutral H_2SO_4 and H_2O molecules. A stable structure of 4c was not found in the present study using the HF method even with more extensive basis sets, e.g., 6-311++G(3df,3p), but the DFT calculation was recreated here at the B3LYP/6-31+G(d) level. One hydrogen atom on H_2O forms a favorable bond with the H_2SO_4 oxygen, (0.99, 160, 1.76), but the bond to the oxygen on H_2O is considerably weaker, (0.98, 145, 2.15). H_2O in this structure is more vibrationally constrained, and using unscaled frequencies,[23,24] the calculated entropy of this structure has the lowest value of all of the $HSO_4^-(H_2O)$ isomers.

$HSO_4^-(H_2SO_4)(H_2O)$. Three isomers of $HSO_4^-(H_2SO_4)(H_2O)$ are shown in Figure 5. The H_2O ligand in structures a and b is bound to the ion by two weak hydrogen bonds of the same type as in the $HSO_4^-(H_2O)$ isomer 4a. The bond lengths and angles of the triply bonded $HSO_4^-(H_2SO_4)$ core in these structures are nearly unperturbed by the presence of one H_2O ligand.[9] Not surprisingly, the two structures, 5a and 5b, have very similar energies and entropies. Structure 5b has C_s symmetry, but the weaker hydrogen bond to the protonated oxygen atom on HSO_4^-, (0.95,129,2.54), gives this structure a slightly higher internal energy than structure 5a . The H_2O ligand in structure 5c is incorporated within the cluster ion, and this geometry allows more favorable hydrogen bonds to form, (0.97,167,1.79) and (0.98,176,1.71). However, the cluster energy is 2.8 kcal mol^{-1} higher than that of 5a due to the loss of one of the strong $HSO_4^-{\cdot}H_2SO_4$ bonds [$\Delta H°$(298 K) = 41.8 kcal mol^{-1} for $HSO_4^-(H_2SO_4) \rightarrow HSO_4^- + H_2SO_4$].[9,10] The two stronger H_2O linkages in 5c give the cluster more rigidity, and the absolute entropy of structure 5c is lower than that of 5a and 5b by 2−3 cal mol^{-1} K^{-1} due to one less low-frequency torsional mode.

$HSO_4^-(H_2SO_4)(H_2O)_2$. Structures 5d and 5e were built from the lowest energy $HSO_4^-(H_2SO_4)(H_2O)$ structure, 5a, by adding another doubly hydrogen-bonded H_2O ligand to the cluster ion.

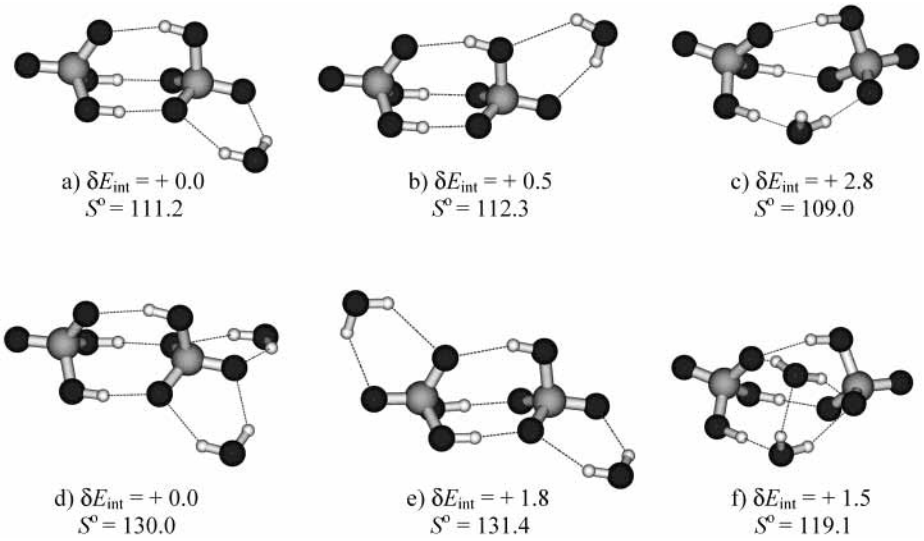

Figure 5. Convergent structures of the $HSO_4^-(H_2SO_4)(H_2O)$ and $HSO_4^-(H_2SO_4)(H_2O)_2$ cluster ions.

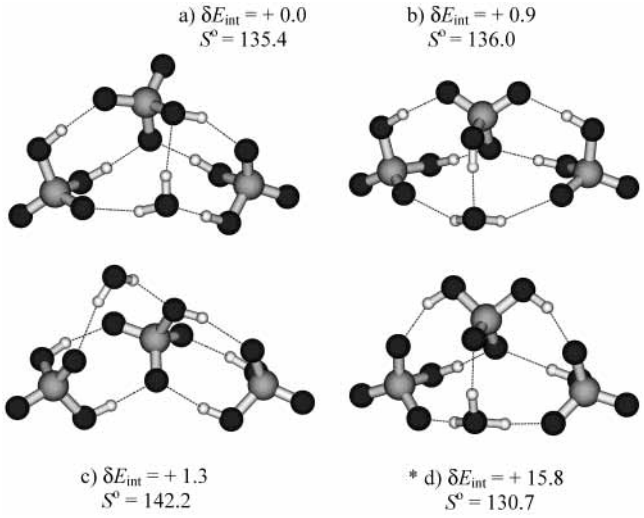

Figure 6. Convergent structures for the $HSO_4^-(H_2SO_4)_2(H_2O)$ cluster ion. * indicates a multiply ionic structure.

The lowest energy structure is the C_s symmetric 5d, with 2 equiv H_2O ligands bound to the HSO_4^- core ion by weak hydrogen bonds with geometries similar to the smaller clusters. Adding the second H_2O ligand instead to the H_2SO_4 molecule results in 5e. This structure is 1.8 kcal mol^{-1} higher in energy because the $H_2SO_4 \cdot H_2O$ hydrogen bonds, (0.95, 136, 2.51) and (0.95, 143, 2.31), do not benefit from the stabilizing ion−dipole forces of the $HSO_4^- \cdot H_2O$ linkages. Force constant calculations yielded 12 vibrational modes with frequencies < 200 cm^{-1} for both 5d and 5e geometries, and the absolute entropy values are within 2 cal mol^{-1} K^{-1}. Structure 5f is built from the $HSO_4^-(H_2SO_4)(H_2O)$ structure in 5c by adding an H_2O ligand that bridges HSO_4^- and H_2SO_4 and forms a hydrogen bond with the free H on the first H_2O. Three new bonds are formed with the addition of this ligand, and all the isomers, 5d, 5e, and 5f, have the same number of hydrogen bonds. The energy of 5f lies between the energies of the two isomers that preserve the triply bonded $HSO_4^-(H_2SO_4)$ arrangement. However, the 5f structure is much more vibrationally constrained; the torsional motions within the cluster occur at higher frequencies (only 9 modes have ν <200 cm^{-1}), resulting in an entropy more than 10 cal mol^{-1} K^{-1} lower than for the most energetically stable isomer, 5d.

$HSO_4^-(H_2SO_4)_2(H_2O)$. The two most stable $HSO_4^-(H_2SO_4)_2(H_2O)$ structures, 6a and 6b in Figure 6, have nearly identical bonding arrangements, a central HSO_4^- ion surrounded by two H_2SO_4 molecules with an H_2O molecule bridging the neutrals and the ion. Both structures possess one favorable hydrogen bond to the oxygen atom of H_2O, (0.98,179,1.71) in 6a and (0.97,176,1.73) in 6b. Both isomers are related to the $HSO_4^-(H_2SO_4)_2$ structure β reported in our previous study,[9] with the H_2O ligand incorporated into the hydrogen bond between the two H_2SO_4 molecules of that structure. The thermal vibrational energy of these clusters, $E_{vib} \approx 7.3$ kcal mol^{-1} at 246 K, is probably large enough for these two structures to readily interconvert. Structure 6c retains the triply bonded character of the $HSO_4^-(H_2SO_4)$ cluster, resembling the α $HSO_4^-(H_2SO_4)_2$ isomer reported in Curtius et al.[9] The total number of hydrogen bonds is the same as in the other isomers of $HSO_4^-(H_2SO_4)_2(H_2O)$, but the H_2O ligand in 6c is bound by only two weak linkages, (0.95, 161, 2.17) and (0.95, 161, 2.31). The energy of 6c is 1.3 kcal mol^{-1} higher than 6a, but structure 6c has an entropy nearly 7 cal mol^{-1} K^{-1} higher due to the additional vibrational freedom of the H_2O ligand. Rearranging protons within the 6b structure yielded 6d, a C_s symmetric cluster ion consisting of one neutral H_2SO_4 and two HSO_4^- ions separated by H_3O^+. This structure was verified to exist at a local minimum on the potential energy surface, but it is nearly 15 kcal mol^{-1} higher in energy than the similar 6b structure. The strong electric field produced between the H_3O^+ and HSO_4^- ions shortens the two symmetric hydrogen bonds, (1.00, 170, 1.58), by 0.6 Å. As a result, structure 6d is more rigid, with an absolute entropy about 5 cal mol^{-1} K^{-1} lower than for 6b.

$HSO_4^-(H_2SO_4)_2(H_2O)_2$. Up to nine hydrogen bonds can form within the $HSO_4^-(H_2SO_4)_2(H_2O)_2$ cluster ion, resulting in many possible conformations. Structures where every hydrogen atom participates in intermolecular bonding have the lowest internal energies, and several of these convergent isomers are shown in Figure 7, parts a−g. The global minimum structure for the $HSO_4^-(H_2SO_4)_2(H_2O)_2$ cluster ion is shown in Figure 7a. The bonding arrangement is similar to $HSO_4^-(H_2SO_4)_2(H_2O)$ in 6a and 6b, with the H_2SO_4 ligands each bound to the central ion by two strong hydrogen bonds and both H_2O ligands incorporated between the H_2SO_4 molecules. The H_2O hydrogen bond geometries range from (0.99,178,1.67) to (0.95,151,2.15). The C_s symmetric structure in 7b is built by adding an H_2O ligand

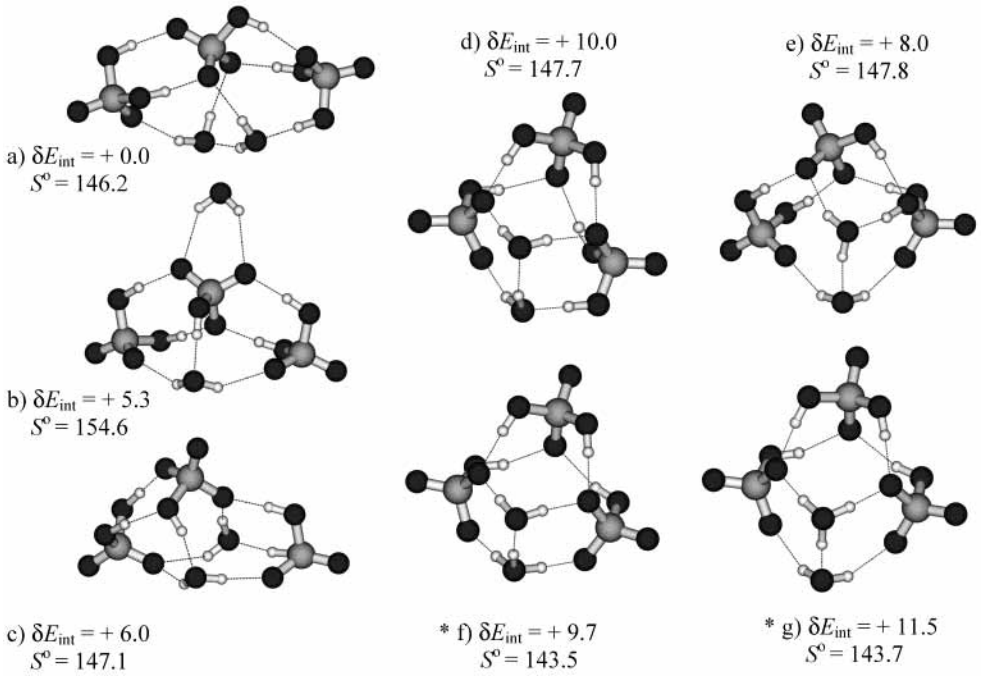

Figure 7. Convergent structures for the $HSO_4^-(H_2SO_4)_2(H_2O)_2$ cluster ion. * indicate a multiply ionic structures.

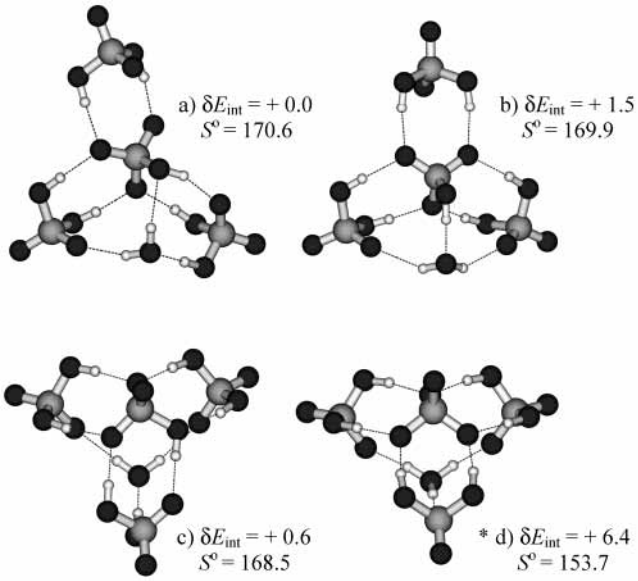

Figure 8. Convergent structures for the $HSO_4^-(H_2SO_4)_3(H_2O)$ cluster ion. * indicates a multiply ionic structure.

to the HSO_4^- ion of 6b via two weak hydrogen bonds, (0.95, 140, 2.34). This H_2O bonding arrangement increases the energy by about 5 kcal mol^{-1} and entropy by about 8 cal mol^{-1} K^{-1} relative to the most stable isomer. In structure 7c, the HSO_4^- core ion is solvated by 5 hydrogen bonds, whereas HSO_4^- in 7a has 6 ligand bonds. Poorer solvation of the core ion and strained H_2O hydrogen bonds in the 7c structure, (0.95, 142, 2.25) and (0.95, 146, 2.22), result in a 6 kcal mol^{-1} higher internal energy than that in 7a. By rearranging protons, many viable isomers can be constructed with the same bonding arrangement as structure 7c, but only the structure shown here was convergent using the HF method.

The four isomers, 7d−7g, are built from a similar geometric framework, and all are significantly higher in energy than the global minimum $HSO_4^-(H_2SO_4)_2(H_2O)_2$ structure 7a. Structures 7d and 7e are singly ionic, but they differ in the placement of the HSO_4^- ion. In the 7d structure, HSO_4^- is poorly solvated by only four hydrogen bonds, with H_2O linkages ranging from (1.00, 177, 1.58) to (0.95, 150, 2.30). The ion in 7e is solvated by one additional hydrogen bond, and consequently, the energy of 7e is 2 kcal mol^{-1} lower than that of 7d. The transfer of one proton in 7d from H_2SO_4 to H_2O results in the multiply ionic 7f isomer, which contains two HSO_4^- ions separated by H_3O^+. The $H_3O^+ \cdot HSO_4^-$ hydrogen bonds in 7f, and in the very similar 7g isomer, are quite favorable, ranging from (1.00, 173, 1.57) to (0.99, 164, 1.66). Both multiply ionic structures have C_s symmetry, but stronger bonds between H_3O^+ and the HSO_4^- ions in 7f result in about a 2 kcal mol^{-1} lower energy. According to relative HF energies, ionization within these isomers does not impose a significant energetic cost: the energies of structures 7d−7g span a range of only 3.5 kcal mol^{-1}. However, stronger electrostatic forces within the H_3O^+-containing structures result in slightly increased rigidity, the entropies of 7f and 7g are 4 cal mol^{-1} K^{-1} lower than those for singly ionic 7d and 7e isomers. Multiply ionic isomers having geometries similar to the minimum energy structure 7a were not convergent.

$HSO_4^-(H_2SO_4)_3(H_2O)$. As with $HSO_4^-(H_2SO_4)_2(H_2O)_2$, there are many possible isomers of the $HSO_4^-(H_2SO_4)_3(H_2O)$ cluster ion: more than 10 local minima on the potential energy surface were found, with cluster energies spanning a range of nearly 20 kcal mol^{-1}. Four of these isomers, representing the most stable and chemically interesting structures, are shown in Figure 8. The lowest energy isomer, structure 8a, is constructed by adding an H_2SO_4 ligand to available oxygen atoms on the central HSO_4^- ion of the $HSO_4^-(H_2SO_4)_2(H_2O)$ structure 6a. However, 8b, similarly built from 6b by adding H_2SO_4 to HSO_4^-, is only 1.5 kcal mol^{-1} higher in energy and has a comparable entropy. The large amount of vibrational energy ($E_{vib} \approx 10.5$ kcal mol^{-1} at 246 K) and similar energies suggest that isomerization may readily populate both 8a and 8b. The 8c isomer has a pinwheel-like structure with a central HSO_4^- ion surrounded by three H_2SO_4 molecules, which are in turn bound to a central H_2O ligand. Hydrogen bonds to the H_2O ligand are highly collinear: (0.95, 176, 1.66), (0.95, 176, 1.98), and (0.95, 173, 2.01). The calculated energy of this structure is within 1 kcal mol^{-1} of

TABLE 2: HF/6-31+G(d) ab Initio Results for the $HSO_4^-(H_2SO_4)_s(H_2O)_w$ Cluster Ion Family[a]

molecule or cluster	structure	E_e	E_{ZP}	E_{int}	$E-E_e$	$H°-E_e$	S°
H_2O		−76.0177	12.79	−47688.34	14.26	14.75	43.45
HSO_4^-		−697.5461	16.50	−437693.66	18.78	19.27	68.63
H_2SO_4		−698.0488	23.74	−438001.86	26.13	26.62	67.48
$HSO_4^-(H_2O)$	4a	−773.5860	31.31	−485393.90	35.16	35.65	85.23
	4b	−773.5863	31.84	−485393.55	35.42	35.91	82.60
	4c	−775.9422	32.18	−486871.53	35.68	36.16	81.12
$HSO_4^-(H_2SO_4)(H_2O)$	5a	−1471.6978	57.08	−923433.31	63.38	63.86	111.21
	5b	−1471.6969	56.97	−923432.86	63.32	63.81	112.26
	5c	−1471.6942	57.52	−923430.59	63.56	64.04	109.03
$HSO_4^-(H_2SO_4)(H_2O)_2$	5d	−1547.7310	71.53	−971129.67	79.62	80.11	129.96
	5e	−1547.7277	71.23	−971127.88	79.38	79.87	131.38
	5f	−1547.7309	73.02	−971128.14	80.31	80.80	119.13
$HSO_4^-(H_2SO_4)_2(H_2O)$	6a	−2169.7925	83.09	−1361461.73	91.85	92.34	135.35
	6b	−2169.7907	82.83	−1361460.82	91.67	92.16	136.01
	6c	−2169.7893	82.34	−1361460.43	91.56	92.05	142.16
	6d*	−2169.7673	83.01	−1361445.98	91.44	91.93	130.74
$HSO_4^-(H_2SO_4)_2(H_2O)_2$	7a	−2245.8322	98.57	−1409161.15	108.57	109.06	146.21
	7b	−2245.8218	97.26	−1409155.91	107.91	108.40	154.57
	7c	−2245.8222	98.29	−1409155.15	108.39	108.88	147.12
	7d	−2245.8153	97.90	−1409151.21	107.99	108.48	147.73
	7e	−2245.8190	98.27	−1409153.17	108.36	108.85	147.79
	7f*	−2245.8173	98.85	−1409151.49	108.48	108.97	143.49
	7g*	−2245.8144	98.84	−1409149.70	108.49	108.97	143.73
$HSO_4^-(H_2SO_4)_3(H_2O)$	8a	−2867.8770	107.95	−1799484.85	119.90	120.39	170.61
	8b	−2867.8745	107.88	−1799483.35	119.81	120.30	169.88
	8c	−2867.8760	107.85	−1799484.34	119.68	120.17	168.52
	8d*	−2867.8681	108.71	−1799478.52	119.67	120.15	153.69

[a] E_e is given in hartrees. E_{ZP}, E_{int}, E, and $H°$are in kcal mol^{-1}, and $S°$ is in cal mol^{-1} K^{-1}. Structures are labeled according to Figures 4 − 8. Thermochemical values are calculated for 246 K. *Denotes multiply ionic structures.

both 8a and 8b, and all three of these structures probably exist in a thermal system.

Structure 8d shares the same pinwheel-like bonding arrangement of 8c, but 8d has C_{3v} symmetry and is multiply ionic. This isomer consists of an SO_4^{2-} central ion surrounded by three neutral H_2SO_4 molecules, which are in turn linked by one H_3O^+ ion. The 8d isomer is only 6.4 kcal mol^{-1} higher in energy than 8a, indicating that very strong solvating bonds, (0.98, 170, 1.68), in 8d help stabilize the charge separation in the cluster. Two other isomers (not shown) with the same bonding arrangement as 8d, but instead containing H_3O^+ and two HSO_4^- ions, had higher relative energies, $\delta E_{int} = 13.4$ and 19.4 kcal mol^{-1}. The absolute entropies of structures 8a−8c span a range of only 2 cal mol^{-1} K^{-1}, but the symmetric 8d isomer has an entropy about 16 cal mol^{-1} K^{-1} lower. A total of 13 torsional modes with frequencies <100 cm^{-1} are associated with the H_2O ligand in structure 8a, constituting more than half the cluster's vibrational entropy. Structure 8d has only 7 such modes that involve H_3O^+. Structures 8c and 8d may be interchanged by the transfer of only two protons. Protonation of the H_2O molecule to give 8d increases the cluster rigidity and significantly lowers the entropy at a relatively small energetic expense.

Discussion

Thermodynamic Measurements. A limited number of equilibrium constants have been measured previously for H_2O association reactions to form $HSO_4^-(H_2SO_4)_s(H_2O)_w$ cluster ions. Thermodynamic measurements from this work are compared to literature values in Figure 9. Böhringer et al. measured equilibrium constants for reaction 1 to form the $HSO_4^-(H_2O)$ product cluster over a 65 K temperature range in a flowing afterglow apparatus.[25] Böhringer also determined an upper limit to $\Delta G°$(300 K) for formation of $HSO_4^-(H_2SO_4)(H_2O)$ of >−3.6 kcal mol^{-1}. Room-temperature measurements were made for $HSO_4^-(H_2O)_w$, $w = 1$ and 2, by Blades et al. using ions produced by electrospray.[26] Extrapolated $HSO_4^-(H_2O)_{1,2}$ van't Hoff lines from the present work overlie the van't Hoff lines of Böhringer and intersect the single temperature results of Blades. Extrapolation of the current van't Hoff data for $HSO_4^-(H_2SO_4)(H_2O)$ is also consistent with the upper limit reported by Böhringer. Arnold et al. estimated $\Delta G°$(233 K) to form the $HSO_4^-(H_2SO_4)_2(H_2O)$, $HSO_4^-(H_2SO_4)_3(H_2O)$, $HSO_4^-(H_2SO_4)_3(H_2O)_2$, and $HSO_4^-(H_2SO_4)_4(H_2O)$ clusters from atmospheric ion measurements using a balloon-borne mass spectrometer.[27] However, these estimations (not shown) are 2.4−3.3 kcal mol^{-1} more negative than $\Delta G°$(233 K) values reported here.

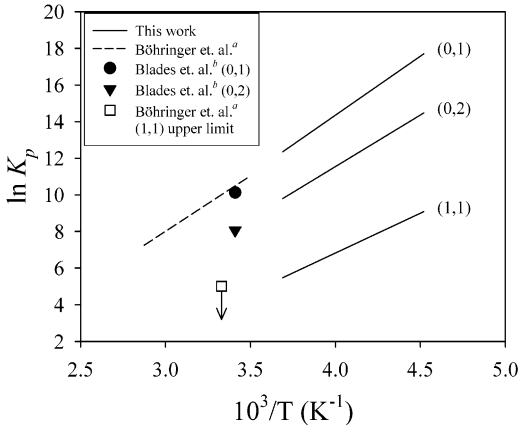

Figure 9. Van't Hoff comparison of laboratory measurements of $HSO_4^-(H_2SO_4)_s(H_2O)_{w-1} + H_2O \rightleftarrows HSO_4^-(H_2SO_4)_s(H_2O)_w$ equilibria. Labels indicate the product cluster (*s*,*w*). [a]Reference 25. [b]Reference 26.

Plots of $\Delta H°$ and $\Delta S°$ versus the number of H_2O ligands for the $HSO_4^-(H_2SO_4)_s(H_2O)_w$ cluster ions are presented in Figure 10. The shapes of the $\Delta H°$ and $\Delta S°$ curves are qualitatively similar, and in general, one would expect a correlation between ligand bond strength and the vibrational rigidity of the cluster. As evident from the mass spectra, the $\Delta H°$ trends in Figure 10

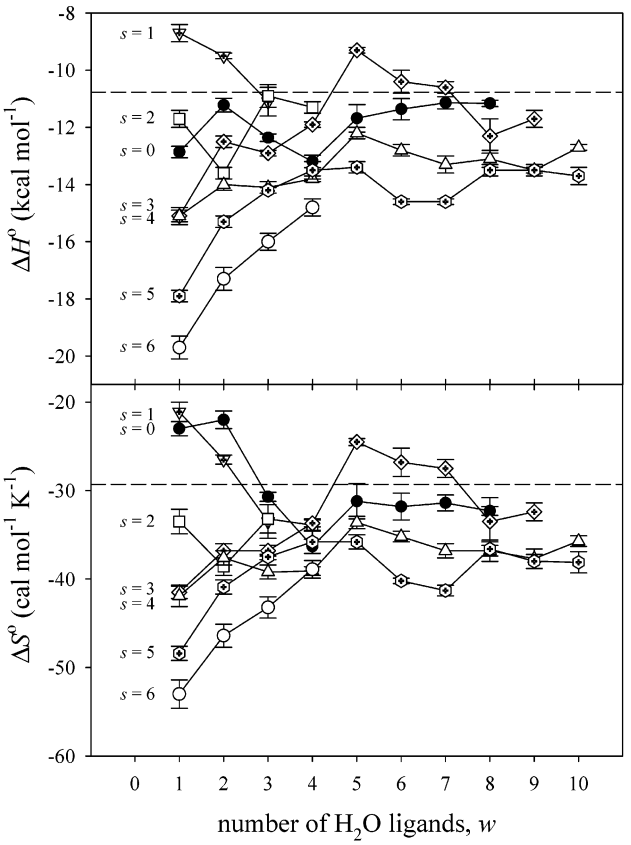

Figure 10. Experimental bond enthalpy and entropy derived from van't Hoff analyses for the reaction, $HSO_4^-(H_2SO_4)_s(H_2O)_{w-1} + H_2O \rightleftarrows HSO_4^-(H_2SO_4)_s(H_2O)_w$, $s = 0-6$. Error bars are one standard deviation of the fit parameter and represent precision only. The dashed lines are $\Delta H^\circ_{cond}(273\ K)$ and $\Delta S^\circ_{cond}(273\ K)$ for bulk water.

show quantitatively that the HSO_4^- ion generally has a higher affinity for H_2O than the slightly larger $s = 1-3$ cluster ion groups but that the $s = 4-6$ clusters again become more hydrophilic. Strong ion−dipole forces between HSO_4^- and H_2O account for the relative stability ($\Delta H^\circ \approx -12$ kcal mol^{-1}) of the first few ligands in $HSO_4^-(H_2O)_w$. The H_2O bond enthalpy for $HSO_4^-(H_2SO_4)(H_2O)$ is -8.7 kcal mol^{-1}, more than 4 kcal mol^{-1} weaker than in $HSO_4^-(H_2O)$, but ΔH° for the $s = 1$ series becomes more favorable with additional H_2O ligands. H_2SO_4 very effectively solvates the HSO_4^- ion, as indicated by the strong bond, large negative reaction entropy ($\Delta S^\circ = -42.6$ cal mol^{-1} K^{-1}),[28] and triply bonded structure of $HSO_4^-(H_2SO_4)$.[9,10] Evidently, the presence of one solvating H_2SO_4 ligand significantly disrupts the electrostatic attraction between HSO_4^- and H_2O. The small negative entropy of association to form both $HSO_4^-(H_2O)$ and $HSO_4^-(H_2SO_4)(H_2O)$ clusters via reaction 1 ($\Delta S^\circ > -25$ cal mol^{-1} K^{-1}) suggests that the H_2O ligand has considerable freedom of motion.

As H_2SO_4 ligands are added to the $HSO_4^-(H_2SO_4)_s(H_2O)_w$ clusters, H_2O becomes more strongly bound. Reaction enthalpy values for the larger $HSO_4^-(H_2SO_4)_3(H_2O)$ and $HSO_4^-(H_2SO_4)_4(H_2O)$ clusters are $\Delta H^\circ \approx -15$ kcal mol^{-1}. The magnitude of ΔS° also increases further for these clusters, indicating significant molecular rearrangement or a more rigidly bound H_2O ligand than in the smaller clusters. The nearly identical ΔH° and ΔS° values to form $HSO_4^-(H_2SO_4)_3(H_2O)$ and $HSO_4^-(H_2SO_4)_4(H_2O)$ suggest very similar bonding for the H_2O ligands in these clusters. In the $s = 3$ series, distinct peaks in both the ΔH° and ΔS° curves at $w = 5$ (Figure 10) coincide with the abrupt change in the shape of the $HSO_4^-(H_2SO_4)_3(H_2O)_w$ cluster ion distribution (Figure 1b). H_2O bond strength continues to increase with additional H_2SO_4 ligands: $\Delta H^\circ = -18.0$ and -19.7 kcal mol^{-1} for $HSO_4^-(H_2SO_4)_5(H_2O)$ and $HSO_4^-(H_2SO_4)_6(H_2O)$, respectively. Interestingly, ΔS° values for these clusters are approximately -50 cal mol^{-1} K^{-1}. Translational and rotational entropy loss in an association reaction typically accounts for about -30 cal mol^{-1} K^{-1}, and the $\sim$20 cal mol^{-1} K^{-1} discrepancy must be due to vibrational entropy loss as H_2O is added to $HSO_4^-(H_2SO_4)_s$, $s = 5$ and 6. Large changes in both enthalpy and entropy suggest that H_2O ligands are incorporated rigidly within the $HSO_4^-(H_2SO_4)_5(H_2O)$ and $HSO_4^-(H_2SO_4)_6(H_2O)$ cluster ions and probably have very different bonding arrangements than in the smaller clusters. Ab initio structures of the $HSO_4^-(H_2SO_4)_s(H_2O)_w$ clusters were calculated to investigate these trends in H_2O ligand bonding, and cluster entropies are discussed in more detail below.

The reaction enthalpy for association of H_2O to the largest observable cluster in each s series is between $\Delta H^\circ = -11$ and -15 kcal mol^{-1}. In the limit of an infinite number of H_2O ligands, ΔH° will converge to the enthalpy of condensation of bulk water, ΔH°_{cond}. The largest H_2O clusters measured in the $s = 0-3$ series are all within 1 kcal mol^{-1} of $\Delta H^\circ_{cond}(273\ K) = -10.8$ kcal mol^{-1}.[29] However, the largest $s = 4-6$ clusters bond H_2O more strongly, analogous to bulk liquid H_2SO_4/H_2O solutions, where the H_2O vapor pressure decreases with increasing H_2SO_4 mole fraction. ΔS° values for the first H_2O ligand on the $HSO_4^-(H_2SO_4)_s$ clusters span a considerable range from -21 to -53 cal mol^{-1} K^{-1}, but as the number of H_2O ligands increases, reaction entropies converge to values between -30 and -40 cal mol^{-1} K^{-1}. The ΔS° results for $HSO_4^-(H_2SO_4)_s(H_2O)_w$, $s = 0-3$, converge to within 3 cal mol^{-1} K^{-1} of $\Delta S^\circ_{cond}(273\ K) = -29.3$ cal mol^{-1} K^{-1} for bulk water,[29] but ΔS° values for the $s \geq 4$ series are markedly more negative. The ΔH° and ΔS° results indicate that H_2SO_4 molecules significantly affect H_2O ligand bonding for a wide range of $HSO_4^-(H_2SO_4)_s(H_2O)_w$ clusters and that, as these cluster ions grow in size, they begin to show thermodynamic trends characteristic of bulk liquids.

Comparison of ab Initio and Experimental Thermodynamics. Accurate cluster ion energies are not an essential result of the current ab initio study, and consequently, MP2 corrections to HF optimized geometries were not determined, and reaction thermochemical values were not corrected for basis set superposition error. Absolute enthalpies for hydrogen-bonded isomers calculated at the HF/6-31+G(d) level have uncertainties of many kcal mol^{-1}, but relative energies (δE_{int}) of individual isomers will be more accurate. This level of theory should predict cluster entropies accurate to within a few cal mol^{-1} K^{-1}. Calculated and experimental reaction enthalpies and entropies for the $HSO_4^-(H_2SO_4)_s(H_2O)_w$ clusters are compared in Table 3.

1. Singly Ionic Structures. Ab initio structures show that HSO_4^- and $HSO_4^-(H_2SO_4)$ cluster ions do not offer favorable binding sites for H_2O ligands. For the most energetically stable $HSO_4^-(H_2O)$, $HSO_4^-(H_2SO_4)(H_2O)$, and $HSO_4^-(H_2SO_4)(H_2O)_2$ structures in Figures 4 and 5, H_2O ligands are loosely bound to the exterior of the cluster, consistent with weak experimental bond enthalpies and low negative reaction entropies. The calculated ΔS° value for formation of $HSO_4^-(H_2O)$ isomer 4a is within 4 cal mol^{-1} K^{-1} of the measured reaction entropy, but the more vibrationally restricted H_2O ligands in structures 4b and 4c result in lower absolute cluster entropies that do not agree with experiment. Structures where H_2O ligands bind to the exterior of the $HSO_4^-\cdot H_2SO_4$ core yield ΔS° values within 5 cal mol^{-1} K^{-1} of the experimental reaction entropies. Although

TABLE 3: Comparison of ab Initio and Experimental Thermochemical Values for the Reactions, $HSO_4^-(H_2SO_4)_s(H_2O)_{w-1} + H_2O \rightleftarrows HSO_4^-(H_2SO_4)_s(H_2O)_w$[a]

product cluster	structure	ΔE_{ai}	$\Delta H°_{ai}$	$\Delta H°_{exp}$	$\Delta S°_{ai}$	$\Delta S°_{exp}$
$HSO_4^-(H_2O)$	4a	−11.8	−12.3	−12.9 (0.6)	−26.8	−23.0 (2.7)
	4b	−11.7	−12.2		−29.5	
	4c				−31.0	
$HSO_4^-(H_2SO_4)(H_2O)$	5a	−8.6	−9.1	−8.7 (0.7)	−25.7	−21.1 (3.0)
	5b	−8.1	−8.6		−24.7	
	5c	−6.2	−6.7		−27.9	
$HSO_4^-(H_2SO_4)(H_2O)_2$	5d	−7.7	−8.2	−9.5 (0.4)	−24.7	−26.5 (1.5)
	5e	−5.8	−6.3		−23.3	
	5f	−7.0	−7.4		−35.5	
$HSO_4^-(H_2SO_4)_2(H_2O)$	6a	−8.7	−9.2	−11.7 (0.9)	−34.3	−33.5 (3.8)
	6b	−7.7	−8.2		−33.6	
	6c	−7.0	−7.5		−27.5	
	6d*	+6.7	+6.2		−38.9	
$HSO_4^-(H_2SO_4)_2(H_2O)_2$	7a	−11.3	−11.8	−13.6 (0.7)	−32.6	−38.6 (2.7)
	7b	−5.4	−5.9		−24.2	
	7c	−5.2	−5.7		−31.7	
	7d	−1.3	−1.8		−31.1	
	7e	−3.2	−3.7		−31.0	
	7f*	−2.0	−2.5		−35.3	
	7g*	−0.2	−0.7		−35.1	
$HSO_4^-(H_2SO_4)_3(H_2O)$	8a	−8.6	−9.1	−15.1 (0.4)	−30.8	−41.5 (1.5)
	8b	−7.1	−7.6		−31.5	
	8c	−8.2	−8.7		−32.9	
	8d*	−3.3	−3.8		−47.7	

[a] ΔE and $\Delta H°$ are given in kcal mol^{-1}, and $\Delta S°$ values are in cal mol^{-1} K^{-1}. Ab initio values were calculated using E, $H°$, and $S°$ from reactant isomers with the lowest internal energy, E_{int}. Thermochemical parameters are calculated at 246 K. Values in parentheses are 95% confidence intervals. * Denotes multiply ionic structures.

stable geometries can be formed by incorporating H_2O ligands into the triply bonded $HSO_4^-(H_2SO_4)$ cluster ion (structures 5c and 5f), these isomers give calculated $\Delta S°$ values 7 and 9 cal mol^{-1} K^{-1} more negative, respectively, than the experimental numbers. As seen previously with the $HSO_4^-(H_2SO_4)_s$ ab initio structures,[9,10] there is surprising quantitative agreement between calculated and experimental $\Delta H°$ values. For the $HSO_4^-(H_2O)$, $HSO_4^-(H_2SO_4)(H_2O)$, and $HSO_4^-(H_2SO_4)(H_2O)_2$ cluster ions, HF ab initio bond enthalpies agree to within 1.5 kcal mol^{-1} with those of the experimental measurements.

For the $HSO_4^-(H_2SO_4)_2(H_2O)$ and larger cluster ions, more ligand binding sites are available. H_2O ligands are not restricted to the less favorable bonding geometries observed in the smaller clusters, and they are frequently bound by three hydrogen bonds. Interligand bonds become more prevalent, and structures with three bonds between HSO_4^- and H_2SO_4 are no longer calculated to be the most stable isomers. The experimental $\Delta S°$ value for formation of the $HSO_4^-(H_2SO_4)_2(H_2O)$ cluster ion is −33.5 cal mol^{-1} K^{-1}, significantly more negative than for those of the smaller cluster ions. Calculated $\Delta S°$ values for isomers 6a and 6b, where H_2O is incorporated into the cluster, are in close agreement with those of the experiment, but the reaction entropy for 6c is 6 cal mol^{-1} K^{-1} less negative because of the loosely bound H_2O. The $HSO_4^-(H_2SO_4)_2(H_2O)_2$ structures are comprised of multiple rings, similar to those observed in ab initio $H_2SO_4(H_2O)_w$ structures,[18,19] which provide greater stability and rigidity. Isomer 7a has the lowest ab initio energy, and the calculated H_2O bond enthalpy is within 2 kcal mol^{-1} of the experimental value. However, the experimental $\Delta S°$ value (−38.6 cal mol^{-1} K^{-1}) is at least 6 cal mol^{-1} K^{-1} more negative than that predicted by any of the singly ionic $HSO_4^-(H_2SO_4)_2(H_2O)_2$ isomers. The three singly ionic $HSO_4^-(H_2SO_4)_3(H_2O)$ isomers shown in Figure 8 have nearly equivalent energies and entropies. These structures are by far the lowest energy species found in a comprehensive search for stable $HSO_4^-(H_2SO_4)_3(H_2O)$ geometries. However, the agreement between calculated and experimental $\Delta H°$ and $\Delta S°$ values is worse than for the smaller clusters. Ab initio H_2O bond enthalpies are more than 6 kcal mol^{-1} weaker, and reaction entropies are ∼10 cal mol^{-1} K^{-1} less negative than measured values.

2. Multiply Ionic Structures. H_3O^+ and HSO_4^- ions represent a significant fraction of bulk H_2SO_4/H_2O solutions.[30] As strong acid−water molecular clusters grow in size, multiple ions become better solvated, and the stability of multiply ionic geometries must eventually surpass that of singly ionic species. The energy required to remove the first proton from an isolated gas-phase H_2SO_4 molecule is ∼310 kcal mol^{-1},[31] 145 kcal mol^{-1} more energy than is gained by adding the proton to H_2O.[32] For proton transfer from H_2SO_4 to H_2O to occur within a molecular cluster, this 145 kcal mol^{-1} of residual energy must be offset by strengthened intermolecular bonds due to ion−ligand solvation and ion−ion electrostatic attraction. Ab initio studies of $H_2SO_4(H_2O)_w$ show that ionization via internal proton transfer from H_2SO_4 to H_2O can yield stable geometries of the form $HSO_4^-\cdot H_3O^+(H_2O)_{w-1}$ for $w \geq 3$,[18,19] and for both $H_2SO_4(H_2O)_w$ and $HCl(H_2O)_w$,[33] the most stable forms of the $w = 5$ cluster are multiply ionic.

In the present study of $HSO_4^-(H_2SO_4)_s(H_2O)_w$ clusters, stable multiply ionic structures were identified for $s = 2$ and 3. HF theory predicts that forming SO_4^{2-} or a second HSO_4^- ion comes at an energetic cost that is not entirely offset by protonation of one H_2O molecule and subsequent solvation of the multiple ions, and the most energetically stable species for all clusters were singly ionic. However, the relative HF energies of multiply ionic species decrease rapidly with increasing cluster size. The multiply ionic $HSO_4^-(H_2SO_4)_2(H_2O)_2$ isomers, 7f and 7g, show better agreement with the experimental reaction entropies than do the singly ionic isomers. None of the individual ab initio $HSO_4^-(H_2SO_4)_3(H_2O)$ structures, 8a−8d, reproduces the experimental entropy. However, in a thermal system, multiple stable isomers will contribute to the measured $\Delta S°$ value according to their relative populations, and a system which includes both singly ionic isomers and the SO_4^{2-}/H_3O^+ isomer

TABLE 4: Derived Enthalpies and Entropies for the Association Reaction, $HSO_4^-(H_2SO_4)_{s-1}(H_2O)_w + H_2SO_4 \rightarrow HSO_4^-(H_2SO_4)_s(H_2O)_w$ Cluster Ions, $s = 1-5$

number of H_2O ligands, w	number of H_2SO_4 ligands, s				
	1	2	3	4	5
		$\Delta H^\circ_{s-1,s}$			
0	−41.8[a]	−27.4[a]	−23.8[a]	−21.6[a]	−20.4[a]
1	−37.6	−30.4	−27.2	−21.5	−23.3
2	−35.9	−34.5	−26.2	−23.1	−24.5
3	−34.6	−34.4	−28.2	−24.2	−24.6
4			−28.9	−26.1	−24.2
		$\Delta S^\circ_{s-1,s}$			
0	−42.6[a]	−34.4[a]	−35.3[a]	−35.7[a]	−34.9[a]
1	−40.7	−46.8	−43.3	−36.2	−41.2
2	−45.3	−58.8	−41.6	−36.9	−44.6
3	−48.2	−58.5	−45.2	−39.3	−42.9
4			−45.0	−44.7	−39.6

[a] Experimental ΔH° results and ab initio ΔS° values from our previous work (Reference 9,10). All other values were determined from thermochemical reaction cycles based on the current measurements.

8d would give an association reaction entropy that better agrees with the experimental value. The comparison of ab initio and experimental reaction entropies for the $HSO_4^-(H_2SO_4)_2(H_2O)_2$ and $HSO_4^-(H_2SO_4)_3(H_2O)$ clusters suggests that multiply ionic isomers may be thermally populated and that, e.g., for $HSO_4^-(H_2SO_4)_3(H_2O)$, partial ionization to 8d lowers the measured thermal entropy. Because multiply ionic clusters are comprised of highly polar interligand bonds, it is likely that HF energies of the multiply ionic species relative to singly ionic isomers (δE_{int}) are less accurate. Higher level ab initio calculations are needed to more accurately determine the relative energetics of singly and multiply ionic $HSO_4^-(H_2SO_4)_s(H_2O)_w$ clusters.

Comparison of Positive and Negative H_2SO_4/H_2O Cluster Ions. In a study of fast atom bombardment of sulfuric acid solutions,[34] positive ion clusters, $H^+(H_2SO_4)_s(H_2O)_w$, were observed with up to three H_2O molecules, whereas no H_2O ligands were found in the negative clusters, $HSO_4^-(H_2SO_4)_s$ for $s \leq 20$. These qualitative observations agree with current findings[11] that the small positive clusters are generally more hydrophilic. Compared to its strong attraction to the H^+ core ion, H_2O exhibits a much weaker affinity toward HSO_4^-, typical of H_2O bonding to weakly basic anions such as HCO_3^- and NO_3^-.[35] H_2SO_4 and H_2O have nearly identical proton affinities,[32] and in small positive clusters, H_2SO_4 seems to resemble a H_2O ligand, having little influence on H_2O bonding thermodynamics. In contrast, H_2SO_4 molecules within the $HSO_4^-(H_2SO_4)_s(H_2O)_w$ cluster ions have a significant impact on H_2O bonding due to strong interactions between H_2SO_4 and the HSO_4^- ion. H_2O ligand bonding to small $HSO_4^-(H_2SO_4)_s$ clusters is initially weak but becomes much more favorable as the HSO_4^- ion is solvated by H_2SO_4. Using $HSO_4^-(H_2SO_4)_s$ thermodynamic values from our previous study[9,10] and those for H_2O ligands presented here, H_2SO_4 bond enthalpies and entropies, $\Delta H^\circ_{s-1,s}$ and $\Delta S^\circ_{s-1,s}$, for the $HSO_4^-(H_2SO_4)_s(H_2O)_w$ binary clusters were determined through thermodynamic reaction cycles. Derived $\Delta H^\circ_{s-1,s}$ and $\Delta S^\circ_{s-1,s}$ values are listed in Table 4. In general, H_2SO_4 ligands are stabilized by addition of H_2O to the cluster ($s > 1$), similar to trends in the positive cluster family, $H^+(H_2SO_4)_s(H_2O)_w$. However, H_2SO_4 ligands in the negative H_2SO_4/H_2O cluster ions are bound more strongly than in the positive clusters, typically by >5 kcal mol^{-1}. As H_2SO_4/H_2O cluster ions grow in size, bulk thermodynamic trends become apparent in both systems. The initial differences between $H^+(H_2SO_4)_s(H_2O)_w$ and $HSO_4^-(H_2SO_4)_s(H_2O)_w$ disappear as the core ions are solvated, and by $(s + w) \geq 8-10$, the clusters have comparable H_2O bonding thermodynamics.

Atmospheric Implications. Mass spectra show that both positive and negative H_2SO_4/H_2O cluster ion families can bind many H_2O ligands under atmospheric conditions. At $T \leq 250$K and RH $\geq$ 30%, broad and well developed equilibrium H_2O distributions form on both $H^+(H_2SO_4)_s$ and $HSO_4^-(H_2SO_4)_s$ clusters. Growth of the positive H_2SO_4/H_2O cluster ions is initially driven by favorable solvation of the proton by H_2O ligands, forming a stable distribution of $H^+(H_2O)_w$ ions. Because H_2O concentrations in the atmosphere are many orders of magnitude higher than those of H_2SO_4, nucleation of cluster ions will be limited by the incorporation of H_2SO_4 molecules. Despite the initial growth in the H_2O coordinate, addition of H_2SO_4 molecules to the positive clusters is not thermodynamically favorable for most atmospheric conditions. For the negative clusters, effective solvation of the HSO_4^- core ion by H_2SO_4 ligands results in a stable $HSO_4^-(H_2SO_4)_s$ backbone, and these species have repeatedly been observed in the atmosphere.[8] Incorporation of H_2O ligands stabilizes these clusters and allows for further growth in the H_2SO_4 coordinate. The low H_2O affinity of the small $HSO_4^-(H_2SO_4)_s(H_2O)_w$ clusters imposes some initial resistance to growth, but strong H_2SO_4 bonding gives this system a significant advantage over $H^+(H_2SO_4)_s(H_2O)_w$ for promoting ion-induced nucleation under atmospheric conditions. This negative polarity preference is consistent with the experiments of Kim et al.,[4] who observed that production of negative particles was favored from charged H_2SO_4/H_2O vapors. Theoretical treatments[36] and other laboratory studies conducted using a variety of compounds[5,37] suggest that polarity preferences in nucleation about ions are due to chemical properties of the precursor gases. In the atmosphere, $HSO_4^-(H_2SO_4)_s(H_2O)_w$ and $H^+(H_2SO_4)_s(H_2O)_w$ clusters may incorporate additional compounds such as NH_3, which is likely to alter the molecular properties of the clusters and may therefore affect the preference for negative ion growth.

Summary

Accurate thermodynamics of the initial stages of cluster ion growth are critical to properly model ion-induced nucleation. Thermodynamics of H_2O binding in the $HSO_4^-(H_2SO_4)_s(H_2O)_w$ cluster ions were measured at tropospheric temperatures and relative humidities, and the complete thermodynamics of stepwise cluster ion growth for this system are now known through $s = 5$. Thermodynamic barriers to incorporation of H_2SO_4 molecules in the analogous positive cluster ions, $H^+(H_2SO_4)_s(H_2O)_w$, limit their ability to attain stable particles sizes, and growth of H_2SO_4/H_2O cluster ions via the negative ion channel is thermodynamically favored. A kinetic model of ion-induced nucleation of the H_2SO_4/H_2O system, which incorporates experimental thermodynamics presented here and in previous works,[9,10] is currently under development in our laboratory.

The weak H_2O bonding measured experimentally for the $HSO_4^-(H_2O)$, $HSO_4^-(H_2SO_4)(H_2O)$, and $HSO_4^-(H_2SO_4)(H_2O)_2$ clusters is well described by ab initio HF/6-31+G(d) calculations. As H_2SO_4 molecules are added, more favorable H_2O binding geometries are made available. H_2O ligands become bound by three or more hydrogen bonds and are further incorporated into the cluster, resulting in stronger H_2O bond enthalpies and larger negative reaction entropies measured for $HSO_4^-(H_2SO_4)_s(H_2O)_w$ as the number of H_2SO_4 ligands is increased. As the clusters become larger, H_2O and H_2SO_4 ligands stabilize one another, analogous to strong acid−water solutions.

Stable multiply ionic structures, $HSO_4^-(HSO_4^-\cdot H_3O^+)(H_2SO_4)_{s-1}(H_2O)_{w-1}$ and $(SO_4^{2-}\cdot H_3O^+)(H_2SO_4)_s$, are calculated for $s = 2$ and 3. The relative HF energies of these isomers suggest that they are not significantly populated in a thermal system. However, the energies of multiply ionic structures become increasingly competitive with singly ionic species as the charge separation is better solvated with additional ligands. Proton transfer within $HSO_4^-(H_2SO_4)_s(H_2O)_w$ cluster ions lowers their absolute entropy, and the large reaction entropy values measured for the $s = 3-6$ clusters may be due to the formation of multiply ionic product clusters. Ab initio calculations of $HSO_4^-(H_2SO_4)_s(H_2O)_w$ cluster ions conducted at higher levels of theory may yield more consistent agreement with experimental bond enthalpies and entropies and may help to better establish the stability of multiply ionic species.

Acknowledgment. The authors acknowledge valuable discussions with J. Curtius, S. Rosen, D. McCabe, P. Marshall, C. J. Howard, and A. R. Ravishankara. We also thank the NOAA Forecast Systems Laboratory for a generous allotment of time on the Jet computer cluster. This work was conducted at the NOAA Aeronomy Lab while K. F. held a CIRES Graduate Research Fellowship and was supported in part by the NOAA Climate and Global Change Program.

Supporting Information Available: Cartesian coordinates, rotational constants, and vibrational frequencies for the ab initio $HSO_4^-(H_2SO_4)_s(H_2O)_w$ cluster ion structures shown in Figures 4−8. This material is available free of charge via the Internet at http://pubs.acs.org.

References and Notes

(1) Arnold, F. *Nature* **1980**, *284*, 610. Arnold, F. *Nature* **1982**, *299*, 134. Turco, R. P.; Zhao, J. X.; Yu, F. Q. *Geophys. Res. Lett.* **1998**, *25*, 635.

(2) Yu, F. Q.; Turco, R. P. *Geophys. Res. Lett.* **2000**, *27*, 883. Yu, F. Q.; Turco, R. P. *J. Geophys. Res.* **2001**, *106*, 4797.

(3) Raes, F.; Janssens, A. *J. Aerosol Sci.* **1986**, *17*, 715. Raes, F.; Janssens, A. *J. Aerosol Sci.* **1985**, *16*, 217. Ramamurthi, M.; Strydom, R.; Hopke, P. K.; Holub, R. F. *J. Aerosol. Sci.* **1993**, *24*, 393. He, F.; Hopke, P. K. *J. Chem. Phys.* **1993**, *99*, 9972. Wood, W. P.; Castleman, A. W.; Tang, I. N. *J. Aerosol Sci.* **1975**, *6*, 367. Bricard, J.; Cabane, M.; Madelaine, G.; Vigla, D. *J. Colloid. Interface Sci.* **1972**, *39*, 42. Kim, T. O.; Ishida, T.; Adachi, M.; Okuyama, K.; Seinfeld, J. H. *Aerosol Sci. Tech.* **1998**, *29*, 111.

(4) Kim, T. O.; Adachi, M.; Okuyama, K.; Seinfeld, J. H. *Aerosol Sci. Tech.* **1997**, *26*, 527.

(5) Adachi, M.; Okuyama, K.; Seinfeld, J. H. *J. Aerosol Sci.* **1992**, *23*, 327.

(6) Yu, F. Q.; Turco, R. P. *Geophys Res. Lett.* **1997**, *24*, 1927. Yu, F. Q.; Turco, R. P. *J. Geophys. Res.* **1998**, *103*, 25915. Yu, F. Q.; Turco, R. P.; Karcher, B.; Schroder, F. P. *Geophys. Res. Lett.* **1998**, *25*, 3839. Yu, F. Q. *Geophys. Res. Lett.* **2001**, *22*, 4191.

(7) Weber, R. J.; Chen, G.; Davis, D. D.; Mauldin, L.; Tanner, D. J.; Eisele, F. L.; Clarke, A. D.; Thorton, D. C.; Bandy, A. R. *J. Geophys. Res.* **2001**, *106*, 24107. Weber, R. J.; McMurry, P. H.; Eisele, F. L.; Tanner, D. J. *J. Atmos. Sci.* **1995**, *52*, 2242.

(8) Arnold, F.; Henschen, G. *Nature* **1978**, *275*, 521. Arijs, E. D.; Nevejans, D.; Frederick, P.; Ingels, J. *Geophys. Res. Lett.* **1981**, *8*, 121. Eisele, F. L. *J. Geophys. Res.* **1989**, *94*, 2183. Eisele, F. L.; Tanner, D. J. *J. Geophys. Res.* **1990**, *95*, 20539. Arnold, F.; Wohlfrom, K. H.; Klemm, M. W.; Schneider, J.; Gollinger, K.; Schumann, U.; Busen, R. *Geophys. Res. Lett.* **1998**, *25*, 2137.

(9) Curtius, J.; Froyd, K. D.; Lovejoy, E. R. *J. Phys. Chem. A* **2001**, *105*, 10867.

(10) Lovejoy, E. R.; Curtius, J. *J. Phys. Chem. A* **2001**, *105*, 10874.

(11) Froyd, K. D.; Lovejoy, E. R. *J. Phys. Chem. A* **2003**, *107*, 9800.

(12) Perry, R. H.; Green, D. W.; Maloney, J. O. *Perry's Chemical Engineers' Handbook*, 7th ed.; McGraw-Hill: New York, 1997.

(13) Rosen, S.; Froyd, K. D.; Curtius, J.; Lovejoy, E. R. *Int. J. Mass. Spectrom.*, submitted for publication, 2003.

(14) Conway, D. C.; Janik, G. S. *J. Chem. Phys.* **1970**, *53*, 1859.

(15) Sunner, J.; Kebarle, P. *J. Phys. Chem.* **1981**, *85*, 327.

(16) Deakyne, C. A. Conventional and unconventional hydrogen-bonded ionic clusters. In *Molecular Interactions*: *from van der Waals to strongly bound complexes*; Scheiner, S., Ed.; John Wiley & Sons: Chichester, U.K., 1997; pp 217. Xantheas, S. S. *Recent Theoretical and Experimental Advances in Hydrogen Bonded Clusters*; Kluwer Academic: Dordrecht, 2000. Deakyne, C. A. *J. Phys. Chem.* **1986**, *90*, 6625. Binning, R. C. *J. Phys. Chem. A* **2000**, *104*, 8097. Cheng, H.-P. *J. Phys. Chem. A* **1998**, *102*, 6201. Frisch, M. J.; Del Bene, J. E.; Binkley, J. S.; Schaefer, J. F. I. *J. Chem. Phys.* **1985**, *84*, 2279. Christie, R. A.; Jordan, K. D. *J. Phys. Chem. A* **2001**, *105*, 7551. Hammam, E.; Lee, E. P. F.; Dyke, J. M. *J. Phys. Chem. A* **2000**, *104*, 4571. Xie, Y.; Remington, R. B.; Schaefer, J. F. I. *J. Chem. Phys.* **1994**, *101*, 4878. Auer, A. A.; Helgaker, T.; Klopper, W. *Phys. Chem. Chem. Phys.* **2000**, *2*, 2235. Lee, E. P. F.; Dyke, J. M. *Mol. Phys.* **1991**, *73*, 375.

(17) Arstila, H.; Laasonen, K.; Laaksonen, A. *J. Chem. Phys.* **1998**, *108*, 1031.

(18) Bandy, A. R.; Ianni, J. C. *J. Phys. Chem. A* **1998**, *102*, 6533.

(19) Re, S.; Osamura, Y.; Morokuma, K. *J. Phys. Chem. A* **1999**, *103*, 3535.

(20) Schmidt, M. W.; Baldridge, K. K.; Boatz, J. A.; Elbert, S. T.; Gordon, M. S.; Jensen, J. H.; Koseki, S.; Matsunaga, N.; Nguyen, K. A.; Su, S. J.; Windus, T. L.; Dupuis, M.; Montgomery, J. A. *J. Comput. Chem.* **1993**, *14*, 1347. Granovsky, A. A. *PC GAMESS, http://classic.chem.msu.su/gran/gamess/index.html*.

(21) Schaftenaar, G.; Noordik, J. H. *J. Comput.-Aided Mol. Des.* **2000**, *14*, 123.

(22) McQuarrie, D. A. *Statistical Mechanics*; Harper Collins: New York, 1976.

(23) Scott, A. P.; Radom, L. *J. Phys. Chem.* **1996**, *100*, 16502.

(24) Bauschlicher, C. W. *Chem. Phys. Lett.* **1995**, *246*, 40.

(25) Bohringer, H.; Fahey, D. W.; Fehsenfeld, F. C.; Ferguson, E. E. *J. Chem. Phys.* **1984**, *81*, 2805.

(26) Blades, A. T.; Klassen, J. S.; Kebarle, P. *J. Am. Chem. Soc.* **1995**, *117*, 10563.

(27) Arnold, F.; Viggiano, A. A.; Schlager, H. *Nature* **1982**, *297*, 371.

(28) $S°(H_2SO_4)$ listed in Curtius et al. is in error due to incorrectly treating H_2SO_4 as a nonsymmetric structure: the correct value is −42.6 rather than −44.0 cal mol^{-1} K^{-1}.

(29) Chase, M. W., Jr. *J. Phys. Chem. Ref. Data* **1998**, *Monograph 9*, 1.

(30) Clegg, S. L.; Brimblecombe, P.; Wexler, A. S. *J. Phys. Chem. A* **1998**, *102*, 2137.

(31) Bartmess, J. E. Negative Ion Energetics Data. In *NIST Chemistry WebBook*; Mallard, W. G., Ed.; National Institute of Standards and Technology: Gaithersburg MD, 2001; Vol. NIST Standard Reference Database Number 69.

(32) Hunter, E. P.; Lias, S. G. *J. Phys. Chem. Ref. Data* **1998**, *27*, 413.

(33) Re, S.; Osamura, Y.; Schaefer, J. F. I. *J. Chem. Phys.* **1998**, *109*, 973.

(34) Sharp, T. R.; Futrell, J. H. *Int. J. Mass Spectrom Ion Process* **1989**, *90*, 39.

(35) Keesee, R. G.; Castleman, A. W. *J. Phys. Chem. Ref. Data* **1986**, *15*, 1011.

(36) Kusaka, I.; Wang, Z.-G.; Seinfeld, J. H. *J. Chem. Phys.* **1995**, *102*, 913. Kusaka, I.; Wang, Z.-G.; Seinfeld, J. H. *J. Chem. Phys.* **1995**, *103*, 8993.

(37) Rabeony, H.; Mirabel, P. *J. Phys. Chem.* **1987**, *91*, 1815. Kane, D.; Daly, G. M.; El-Shall, M. S. *J. Phys. Chem.* **1995**, *99*, 7867.